An improved tensorial implementation of the incremental harmonic balance method for frequency-domain stability analysis

Suguang Dou

DTU Wind Energy, Technical University of Denmark, Frederiksborgvej 399, 4000 Roskilde, Denmark
sudou@dtu.dk

Abstract. Previous studies have proposed a tensor-based implementation of the incremental harmonic balance (IHB) method for gradient-based structural optimization of nonlinear forced resonance and nonlinear normal modes. Here the original implementation is improved for realizing an accurate stability analysis in frequency domain. This improvement is motivated by the unaddressed problem that an accurate stability analysis often requires more harmonics than an accurate response analysis. The proposed improvement helps to reduce the number of harmonics required for an accurate stability analysis and therefore reduce the computational expense. The improved implementation is applied to a nonlinear finite element model of a clamped-clamped beam. The insight gained in this study may be used in other variants of the harmonic balance methods.

Keywords: Nonlinear dynamics, Harmonic balance, Stability, Floquet exponents, Tensorial implementation

1 Introduction

In recent years, there has been a renewed academic interest in the frequency-domain stability analysis of the time-periodic response of the dynamical systems [1,2,3,4]. The frequency-domain stability analysis is based on the Hill method, which combines the Floquet theory and the Fourier series expansion. One problem in frequency-domain stability analysis is related to spurious eigenvalues. In [1], Lazarus and Thomas proposed a criterion to sort the most converged eigenvalues, and validated it in a framework where the harmonic-balance method (HBM) is combined with the asymptotic numerical method (ANM) for path-following or continuation of the response. However, even with a proper sorting criterion, Soykov and Ribeiro reported in [2] that an accurate frequency-domain stability analysis can require more harmonics than an accurate response analysis. This unaddressed problem has motivated the study in this work.

This study is performed in the framework of a tensorial implementation of the incremental harmonic balance (IHB) method. The original implementation

was applied to structural optimization problems for tailoring the nonlinear resonances [5]. In a later study, the tensorial implementation of the IHB method is combined with the alternating frequency/time domain method to study structural optimization problems for tuning the frequency-amplitude dependence of nonlinear normal modes in the context of frame structures [6]. Based on the existing tensorial implementation of the IHB method, the work in this paper investigates the frequency-domain stability analysis and suggests an important improvement in the implementation.

2 Methodology

2.1 Time-domain equations of motion

Consider a mechanical system with geometric nonlinearity. By using the nonlinear finite element models, the time-domain equations of motion can be written as

$$\mathbf{M}\frac{\mathrm{d}^2\mathbf{u}}{\mathrm{d}t^2} + \mathbf{C}\frac{\mathrm{d}\mathbf{u}}{\mathrm{d}t} + \mathbf{g}(\mathbf{u}) = \mathbf{f}(\omega t) \tag{1}$$

where $\mathbf{M}$ is the mass matrix, $\mathbf{C}$ is the damping matrix, $\mathbf{g}$ is the internal force which is a nonlinear function of $\mathbf{u}$, $\mathbf{f}$ is the time-periodic external force, t is the time, and $\omega = 2\pi/T$ is the circular frequency with T denoting the time period. Since the linear stiffness term is treated as a part of the nonlinear internal force $\mathbf{g}$, it is not explicitly shown in the above equation.

In the incremental harmonic balance method, a new scale of time is introduced as $\tau = \omega t = 2\,\pi(t/T)$. By using the new time scale τ, the time-domain equations of motion in Eq. (1) becomes

$$\omega^2\,\mathbf{M}\frac{\mathrm{d}^2\mathbf{u}}{\mathrm{d}\tau^2} + \omega\,\mathbf{C}\frac{\mathrm{d}\mathbf{u}}{\mathrm{d}\tau} + \mathbf{g}(\mathbf{u}) = \mathbf{f}(\tau) \tag{2}$$

2.2 Frequency-domain equations of motion

The incremental harmonic balance method is applied to Eq. (2) through a few steps. First, a Fourier basis is introduced to project the time-domain response into the frequency domain as

$$\mathbf{u}(\tau) = \mathbf{s}(\tau)\,\mathbf{q} \tag{3}$$

where $\mathbf{s}(\tau)$ is a row vector of Fourier basis consisting of the sine and cosine functions, and $\mathbf{q}$ is a column vector of Fourier coefficients which represent the frequency-domain response.

Substituting Eq. (3) into Eq. (2) and applying the Galerkin method, a system of nonlinear equations are obtained as [5]

$$\left(\omega^2\,\overline{\mathbf{M}} + \omega\,\overline{\mathbf{C}}\right)\,\mathbf{q} + \overline{\mathbf{g}}\,(\,\mathbf{q}\,) = \overline{\mathbf{f}} \tag{4}$$

where $\overline{\mathbf{M}}$, $\overline{\mathbf{C}}$, $\overline{\mathbf{g}}$ and $\overline{\mathbf{f}}$ denote the frequency-domain counterpart of the mass matrix, the damping matrix, the internal force, and external force, respectively. For the convenience of communication, we refer to Eq. (4) as the frequency-domain governing equation. Eq. (4) can also be written in a more general form as

$$\mathbf{r}(\mathbf{q}, \omega) = \mathbf{0} \tag{5}$$

where

$$\mathbf{r}(\mathbf{q}, \omega) = \left(\omega^2 \overline{\mathbf{M}} + \omega \overline{\mathbf{C}}\right) \mathbf{q} + \overline{\mathbf{g}}(\mathbf{q}) - \overline{\mathbf{f}} \tag{6}$$

2.3 Response analysis

Since the frequency-domain governing equation is nonlinear, Newton-Raphson method is applied in the incremental harmonic balance method to solve the frequency-domain response. Consider a known solution represented by $\mathbf{q}_0$ and ω_0. An unknown solution in the neighborhood of $\mathbf{q}_0$ and ω_0 can be expressed as

$$\mathbf{q} = \mathbf{q}_0 + \Delta\mathbf{q}, \quad \omega = \omega_0 + \Delta\omega. \tag{7}$$

where $\Delta\mathbf{q}$ and $\Delta\omega$ are the increments of response and frequency, respectively. Substituting Eq. (7) into Eq. (5), we have

$$\mathbf{r}(\mathbf{q}_0 + \Delta\mathbf{q},\ \omega_0 + \Delta\omega) = \mathbf{0} \tag{8}$$

Expanding Eq. (8) at $\mathbf{q}_0$ and ω_0 and retaining the first-order approximation, an incremental form of the frequency-domain governing equation is obtained as

$$\mathbf{K}_q \Delta\mathbf{q} + \mathbf{K}_\omega \Delta\omega = -\mathbf{r}(\mathbf{q}_0, \omega_0) \tag{9}$$

where

$$\mathbf{K}_q = \left.\frac{\partial \mathbf{r}(\mathbf{q}, \omega)}{\partial \mathbf{q}}\right|_{\mathbf{q}=\mathbf{q}_0,\, \omega=\omega_0,} \tag{10a}$$

$$\mathbf{K}_\omega = \left.\frac{\partial \mathbf{r}(\mathbf{q}, \omega)}{\partial \omega}\right|_{\mathbf{q}=\mathbf{q}_0,\, \omega=\omega_0.} \tag{10b}$$

Substituting Eq. (6) into Eqs. (11a) and (11b), we have

$$\mathbf{K}_q = \omega_0^2 \overline{\mathbf{M}} + \omega_0 \overline{\mathbf{C}} + \overline{\mathbf{K}}_t(\mathbf{q}_0), \tag{11a}$$

$$\mathbf{K}_\omega = 2\omega_0 \overline{\mathbf{M}} + \overline{\mathbf{C}}. \tag{11b}$$

where

$$\overline{\mathbf{K}}_t(\mathbf{q}_0) = \left.\frac{\partial \overline{\mathbf{g}}(\mathbf{q})}{\partial \mathbf{q}}\right|_{\mathbf{q}=\mathbf{q}_0} \tag{12}$$

Eq. (9) can be solved with the quantities in Eqs. (11a–12), and a continuation approach such as the arc-length method [5].

2.4 Stability analysis

The local stability of the obtained time-periodic response $\mathbf{u}_0$ is studied by adding a small disturbance $\boldsymbol{\delta}$:

$$\mathbf{u} = \mathbf{u}_0 + \boldsymbol{\delta} \tag{13}$$

Substituting Eq. (13) into Eq. (2) and retaining the first-order approximation, the following equation is obtained as

$$\omega_0^2 \, \mathbf{M} \frac{\mathrm{d}^2 \boldsymbol{\delta}}{\mathrm{d}\tau^2} + \omega_0 \, \mathbf{C} \frac{\mathrm{d}\boldsymbol{\delta}}{\mathrm{d}\tau} + \mathbf{K}_t(\mathbf{q}_0) \, \boldsymbol{\delta} = \mathbf{0} \tag{14}$$

In order to study the frequency-domain stability, the disturbance $\boldsymbol{\delta}$ is assumed as

$$\boldsymbol{\delta} = e^{\lambda \tau} \mathbf{s} \, \mathbf{p} \tag{15}$$

where λ and $\mathbf{p}$ denote the Floquet exponent and vector, respectively.

The first- and second-order derivatives of $\boldsymbol{\delta}$ are

$$\frac{\mathrm{d}\boldsymbol{\delta}}{\mathrm{d}\tau} = \lambda \, e^{\lambda \tau} \mathbf{s} \, \mathbf{p} + e^{\lambda \tau} \frac{\mathrm{d}\mathbf{s}}{\mathrm{d}\tau} \mathbf{p} \tag{16a}$$

$$\frac{\mathrm{d}^2 \boldsymbol{\delta}}{\mathrm{d}\tau^2} = \lambda^2 e^{\lambda \tau} \mathbf{s} \, \mathbf{p} + 2\lambda e^{\lambda \tau} \frac{\mathrm{d}\mathbf{s}}{\mathrm{d}\tau} \mathbf{p} + e^{\lambda \tau} \frac{\mathrm{d}^2 \mathbf{s}}{\mathrm{d}\tau^2} \mathbf{p} \tag{16b}$$

Substituting Eqs. (15–16b) into Eq. (14) and applying the Galerkin method, a quadratic eigenvalue problem is obtained as

$$\left(\mathbf{J}_2 \lambda^2 + \mathbf{J}_1 \lambda + \mathbf{J}_0 \right) \mathbf{p} = \mathbf{0} \tag{17}$$

where

$$\mathbf{J}_0 = \mathbf{K}_q(\mathbf{q}_0, \omega_0), \tag{18a}$$

$$\mathbf{J}_1 = 2 \, \omega_0^2 \, \mathbf{M} \otimes \mathbf{h}^{(1)} + \omega_0 \, \mathbf{C} \otimes \mathbf{h}^{(2)}, \tag{18b}$$

$$\mathbf{J}_2 = \omega_0^2 \, \mathbf{M} \otimes \mathbf{h}^{(2)}. \tag{18c}$$

Here the quantities of $\mathbf{h}^{(1)}$ and $\mathbf{h}^{(2)}$ are given in the following section. The quadratic eigenvalue problem in Eq. (17) can be directly solved. Alternatively, it can be re-written into a linear eigenvalue problem [2].

3 Tensorial implementation

Let N_H denote the highest-order of the retained harmonics. The quantities $\mathbf{h}^{(0)}$, $\mathbf{h}^{(1)}$ and $\mathbf{h}^{(2)}$ are defined as

$$\mathbf{h}^{(0)} = -\frac{1}{2}\begin{bmatrix} 0 & \mathbf{0} & \mathbf{0} \\ \mathbf{0} & \widehat{\mathbf{I}} & \mathbf{0} \\ \mathbf{0} & \mathbf{0} & \widehat{\mathbf{I}} \end{bmatrix}, \quad \widehat{\mathbf{I}} = \begin{bmatrix} 1 & & \\ & \ddots & \\ & & N_H^2 \end{bmatrix}_{N_H \times N_H} \tag{19a}$$

$$\mathbf{h}^{(1)} = \frac{1}{2}\begin{bmatrix} 0 & \mathbf{0} & \mathbf{0} \\ \mathbf{0} & \mathbf{0} & \overline{\mathbf{I}} \\ \mathbf{0} & -\overline{\mathbf{I}} & \mathbf{0} \end{bmatrix}, \quad \overline{\mathbf{I}} = \begin{bmatrix} 1 & & \\ & \ddots & \\ & & N_H \end{bmatrix}_{N_H \times N_H} \tag{19b}$$

$$\mathbf{h}^{(2)} = \frac{1}{2}\begin{bmatrix} 2 & \mathbf{0} & \mathbf{0} \\ \mathbf{0} & \mathbf{I} & \mathbf{0} \\ \mathbf{0} & \mathbf{0} & \mathbf{I} \end{bmatrix}, \quad \mathbf{I} = \begin{bmatrix} 1 & & \\ & \ddots & \\ & & 1 \end{bmatrix}_{N_H \times N_H} \tag{19c}$$

The frequency-domain counterparts of the mass and damping matrices, and the internal and external forces are computed as

$$\overline{\mathbf{M}} = \mathbf{M} \otimes \mathbf{h}^{(0)}, \tag{20a}$$

$$\overline{\mathbf{C}} = \mathbf{C} \otimes \mathbf{h}^{(1)}, \tag{20b}$$

$$\overline{\mathbf{g}} = \begin{bmatrix} \mathbf{h}^{(2)}\,\mathcal{G}_1 \\ \vdots \\ \mathbf{h}^{(2)}\,\mathcal{G}_{N_{dof}} \end{bmatrix}, \tag{20c}$$

$$\overline{\mathbf{f}} = \begin{bmatrix} \mathbf{h}^{(2)}\,\mathcal{F}_1 \\ \vdots \\ \mathbf{h}^{(2)}\,\mathcal{F}_{N_{dof}} \end{bmatrix}, \tag{20d}$$

where $\otimes$ stands for Kronecker product, $\mathcal{G}_i$ and $\mathcal{F}_i$ denote the Fourier coefficients of the internal and external forces for the i^{th} degree of freedom.

The frequency-domain counterpart of the tangent stiffness matrix, $\overline{\mathbf{K}}_t$, is obtained with the assistance of a three-dimensional tensor $\mathbf{h}^{(3)}$ and the operation of tensor contraction.

$$\overline{\mathbf{K}}_t = \begin{bmatrix} \mathbf{h}^{(3)} : \mathcal{K}_{1,1} & \dots & \mathbf{h}^{(3)} : \mathcal{K}_{1,N_{dof}} \\ \vdots & \ddots & \vdots \\ \mathbf{h}^{(3)} : \mathcal{K}_{N_{dof},1} & \dots & \mathbf{h}^{(3)} : \mathcal{K}_{N_{dof},N_{dof}} \end{bmatrix} \tag{21}$$

where : denotes a tensor contraction operation, and $\mathcal{K}_{i,j}$ denotes a vector of Fourier coefficients corresponding to the component at the position $(i,\ j)$ of $\mathbf{K}_t(\mathbf{u}(\tau))$.

In Eq. (21), $\mathbf{h}^{(3)}$ is a three-dimension tensor. The tensor contraction operation of this three-dimension tensor, $\mathbf{h}^{(3)}$, and a vector of Fourier coefficients, $\mathcal{K}_{i,j}$, leads to a two-dimensional matrix of the size $(2N_H+1)\times(2N_H+1)$.

4 Numerical Implementation and Results

4.1 Three-dimension tensor

In the original numerical implementation [5], this three-dimension tensor is defined as

$$\mathbf{h}^{(3)}(i,j,k)=\frac{1}{2\pi}\int_0^{2\pi}\mathcal{S}_i(\tau)\mathcal{S}_j(\tau)\mathcal{S}_k(\tau)\,\mathrm{d}\tau \tag{22}$$

where $\mathcal{S}_i(\tau)$ denote the i^{th} function in a vector $\mathcal{S}$ of cosine and sine functions sorted as

$$\mathcal{S}=[1\quad \cos(\tau)\ \ldots\ \cos(N_H\tau)\quad \sin(\tau)\ \ldots\ \sin(N_H\tau)] \tag{23}$$

and the indices $i,\ j,\ k$ are given as

$$i,j,k=1,\ldots,2N_H+1 \tag{24}$$

In the improved numerical implementation, this three-dimension tensor is defined as

$$\mathbf{h}^{(3)}(i,j,k)=\frac{1}{2\pi}\int_0^{2\pi}\mathcal{S}_i(\tau)\mathcal{S}_j(\tau)\widehat{\mathcal{S}}_k(\tau)\,\mathrm{d}\tau \tag{25}$$

where $\widehat{\mathcal{S}}$ is given as

$$\widehat{\mathcal{S}}=[1\quad \cos(\tau)\ \ldots\ \cos(2N_H\tau)\quad \sin(\tau)\ \ldots\ \sin(2N_H\tau)] \tag{26}$$

and the indices $i,\ j,\ k$ are given as

$$i,j=1,\ldots,2N_H+1,\quad k=1,\ldots,4N_H+1. \tag{27}$$

Note that the size of the three-dimension tensor in Eq. (22) is $(2N_H+1)\times(2N_H+1)\times(2N_H+1)$, whereas the three-dimension tensor in Eq. (**??**) is $(2N_H+1)\times(2N_H+1)\times(4N_H+1)$.

One way to visualize the three-dimension tensor $\mathbf{h}^{(3)}$ is to project it into two-dimension plane, see Figure 1. The harmonics in the first two dimensions are more thoroughly coupled in the improved tensor in Eq. (**??**) in than in the original tensor in Eq. ((22)).

The operation of tensor contraction and a similar definition of the three-dimension tensor was also used in a recent study of the Galerkin averaging-incremental harmonic balance method [7].

The importance of this improvement can be seen from both theoretical and numerical points of view. From theoretical point of view, this improvement enables to accurately compute the frequency counterpart of the tangent stiffness matrix $\overline{\mathbf{K}}_t$ for polynomial nonlinearity up to cubic order. For the cubic nonlinearity, its tangent stiffness is in quadratic form. When the harmonics of the response is up to the order of N_H, the harmonics of the tangent stiffness of the cubic nonlinearity is up to the order of $2N_H$. In the original implementation, the $2N_H$ harmonics in the tangent stiffness is truncated to the order of N_H. In the new implementation with the improvement, the $2N_H$ harmonics of the tangent stiffness are fully used in the computation without truncation. From numerical point of view, this reduces the number of harmonics required to achieve a converged and accurate analysis of response and stability. Without this improvement, the original implementation requires a large value of N_H, which is larger than the highest order of the significant harmonics in the response, to ensure the convergence and accuracy of the results. For the nonlinear finite element example shown later in the numerical results, the significant harmonic in the response is the fundamental harmonic. The original implementation without the improvement can not converge with $N_H = 1$ around the resonance peak. However, the new implementation with the improvement can converge smoothly and efficiently with $N_H = 1$. This

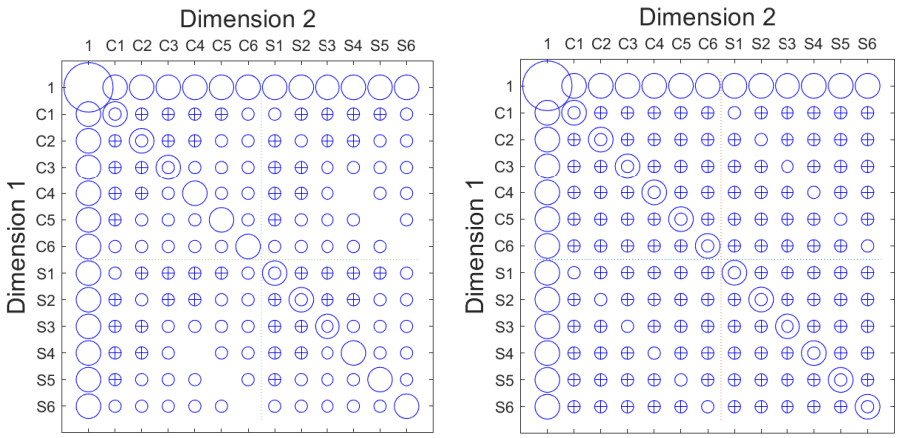

Fig. 1. Visualization of the original and the improved three-dimension tensor $\mathbf{h}^{(3)}$ in a two-dimension plane. $N_H = 6$. Left: the original tensor. Right: the improved tensor. A circle or a cross indicates there is a non-zero value along the third dimension. The size of the circle or cross is proportional to the magnitude of the value in the tensor. $\mathtt{C}n$ and $\mathtt{S}n$ denote the n^{th} order cosine and sine function, respectively.

4.2 Stability analysis

The improved implementation is applied to a finite element model of a clamped-clamped beam with geometric nonlinearity [5]. The beam is discretized into 20 Euler-Bernoulli beam elements. The quadratic and cubic nonlinearity is included to account for the midplane stretching effect [8]. The material properties are given as: Young's modulus $E = 205$ Gpa, and mass density $\rho = 7800$ Kg/m^3. The cross section is a solid square with 0.01m$\times$ 0.01m, and the beam length is $L = 150\sqrt{I/A}$, where A and I denote the area and the second moment of area, respectively. The damping matrix is proportional to the mass matrix, i.e. $\mathbf{C} = \alpha\mathbf{M}$, where $\alpha = 15.58$, leading to a modal damping ratio of 1% for the fundamental flexural mode. The load is applied at the three nodes around the midspan with a magnitude of 10.12 N.

In order to avoid spurious Floquet exponents, a set of $4N_{dof}$ Floquet exponents with the smallest magnitude of the imaginary part are selected. When the reliable Floquet exponents are determined, they are used to estimate the stability of the time-periodic response. A time-periodic response is unstable when there is at least one selected Floquet exponent whose real part is positive

$$\mathrm{Re}(\lambda_i) > 0 \tag{28}$$

Figure 2 shows the response and stability computed by using the improved tensorial implementation. It can be seen that a small number of harmonics ($N_H \geq 2$) is sufficient to realize an accurate stability analysis. This efficiency is attributed to the proposed improvement in the tensorial implementation.

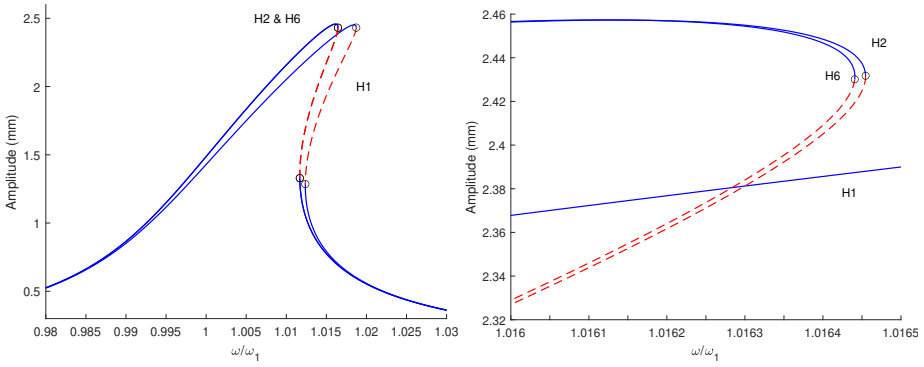

Fig. 2. Nonlinear frequency response of a nonlinear FE model of a clamped-clamped beam. Left: The resonance response at the lowest eigenfrequency. Right: Zoom of the resonance peaks. The solid and the dashed line indicate the stable and unstable response, respectively. The circles indicate the locations of bifurcations. The text $\mathtt{h}n$ indicates the number of harmonics.

5 Conclusions

This paper presents an improved tensorial implementation of the incremental harmonic balance method in [5,6]. The improvement enables an efficient and accurate frequency-domain stability analysis with a small number of harmonics. The proposed implementation is demonstrated by using a finite element model of a clamped-clamped beam with geometric nonlinearity.

The insight gained in this study may be used in other variants of the harmonic balance method. The essence of the proposed improvement is to account for the higher-order ($\geq N_H$) harmonics in the Jacobian matrix that may be truncated in the implementation. These higher-order harmonics are more important for the frequency-domain stability analysis than for the frequency-domain response analysis.

Further study is required to reduce the computational cost of the frequency-domain stability analysis by using advanced model order reduction techniques.

References

1. Lazarus, A., Thomas, O: A harmonic-based method for computing the stability of periodic solutions of dynamical systems. Comptes Rendus Mécanique **338**, 510–517 (2010)
2. Stoykov, S., Ribeiro P.: Stability of nonlinear periodic vibrations of 3D beams. Nonlinear Dyn. **66**, 335–353 (2011)
3. Traversa F.L., Bonani F.: Improved harmonic balance implementation of Floquet analysis for nonlinear circuit simulation. Int. J. Electron. Commun. **66**, 357–363 (2012)
4. Detroux, T., Renson, L., Masset, L., Kerschen, G.: The harmonic balance method for bifurcation analysis of large-scale nonlinear mechanical systems. Comput. Methods Appl. Mech. Eng. **296** 18–38 (2015)
5. Dou S., Jensen J.S.: Optimization of nonlinear structural resonance using the incremental harmonic balance method. *J. Sound Vib.* **334**, 239–254 (2015)
6. Dou S., Jensen J.S.: Optimization of hardening/softening behavior of plane frame structure using nonlinear normal modes. Comput. Struct. **164**, 63–74 (2016)
7. Ju, R., Fan, W., Zhu, W.: An efficient galerkin averaging-incremental harmonic balance method based on the fast Fourier transform and tensor contraction. J. Acoust. Vib. **142** (2020)
8. Chen, S.H., Cheung, Y.K., Xing, H.X.: Nonlinear vibration of plane structures by finite element and incremental harmonic balance method. Nonlinear Dyn. **26**, 87–104 (2001)